

See discussions, stats, and author profiles for this publication at: <https://www.researchgate.net/publication/244465817>

Vapor–Liquid Equilibria for the 1,1,1,2–Tetrafluoroethane (HFC134a) + n Butane (R–600) System

ARTICLE *in* JOURNAL OF CHEMICAL & ENGINEERING DATA · JULY 2007

Impact Factor: 2.04 · DOI: 10.1021/jc700041v

CITATIONS

14

READS

13

4 AUTHORS, INCLUDING:



Jong Sung Lim

Sogang University

143 PUBLICATIONS 1,382 CITATIONS

SEE PROFILE



Gimyeong Seong

Tohoku University

12 PUBLICATIONS 82 CITATIONS

SEE PROFILE

Vapor–Liquid Equilibria for the 1,1,1,2-Tetrafluoroethane (HFC-134a) + *n*-Butane (R-600) System

Jong Sung Lim,* Gimyeong Seong, and Hee-Kook Roh

Department of Chemical and Biomolecular Engineering, Sogang University, C.P.O. Box 1142, Seoul 100-611, South Korea

Hun-Soo Byun

Department of Chemical System Engineering, Chonnam National University, Yosu, Jeonnam 550-749, South Korea

Isothermal vapor–liquid equilibrium data for the binary mixture of 1,1,1,2-tetrafluoroethane (HFC-134a) + normal butane (R600) were measured at 273.15, 283.15, 293.15, 303.15, 313.15, and 323.15 K, respectively. The experiments were carried out using a continuous circulation-type equilibrium apparatus to measure temperature, pressure, and the compositions of the liquid and vapor phases. The experimental data were correlated with the Peng–Robinson equation of state (PR EOS) using the Wong–Sandler (W–S) mixing rule. Calculated results showed good agreement with experimental data. It was found that this system has very strong positive azeotropes for all the temperature ranges studied here.

1. Introduction

After having announced the restriction of using CFCs in Montréal and Kyoto, many advanced countries made a great effort to find replacements for CFCs. Although many countries tried to reduce the use of CFCs, the emission of CFCs has increased nearly twice as high as forecasted. Therefore, finding the proper replacement of CFCs should be accelerated by many scientists and engineers. In view of the situation, mixing HFCs and HCs is a good solution for developing new refrigerants in the near future. Vapor–liquid equilibrium (VLE) data are one of the most important types of information required to evaluate the performance of refrigeration cycles and to determine their optimal compositions. Azeotropic mixtures also have merit because their behaviors are similar to pure compounds. However, very few experimental data have been reported previously in the literature.^{1–4}

In this work, VLE data for a binary mixture of HFC-134a + *n*-butane at five equally spaced temperatures between 273.15 and 323.15 K were measured by using a circulation-type equilibrium apparatus. The experimental data were correlated with the Peng–Robinson equation of state (PR EOS)⁵ using the Wong–Sandler (W–S) mixing rule⁶ combined with the nonrandom two-liquid (NRTL) excess Gibbs free-energy model. Almost all the calculated values with this model give good agreement with the experimental data, and this system exhibits azeotropes.

2. Experimental Section

2.1. Chemicals. High-grade chemicals of HFC-134a and *n*-butane were used for VLE measurement. HFC-134a was supplied by INEOS FLUOR Japan Limited (JAP) with a purity of higher than 99.98 mass %. *n*-Butane was supplied by MG Industry (UK) with a purity of higher than 99.5 % mass. The purities of the chemicals were guaranteed from the manufacturers, and they were used without any further purification.

2.2. Experimental Apparatus. A schematic diagram of the experimental apparatus for measuring the VLE is given in Figure 1. Because the vapor–liquid equilibrium apparatus used in this work is the same as that used in our previous work,^{7–13} it is only briefly described here. It was a circulation-type apparatus in which both liquid and vapor phases were recirculated continuously. The equilibrium cell is a type-316 stainless steel vessel within an inner volume of about 85 cm³. In its middle part, two Pyrex glass windows of 20 mm thickness were installed in front and behind so that the liquid level, mixing and circulating behaviors, and critical phenomena could be observed by a back light during operation. A stirrer, rotated at variable speeds by an external magnet, was used to accelerate the attainment of the equilibrium state and to reduce concentration gradients in both phases.

The temperature of the equilibrium cell in the water bath was maintained by a circulator from Jeio Tech, Korea. The temperature in the cell was measured with a platinum resistance sensor and a digital temperature indicator, model F250MkII, precision thermometer from Automatic Systems Laboratories, Ltd., United Kingdom. They were calibrated by the National Measurement Accreditation Service accredited calibration laboratory. The total uncertainty in temperature measurements is estimated to be within 0.01 K, including sensor uncertainty, temperature resolution, 0.001 K, and measurement uncertainty, 0.001 K. The pressure was measured with a pressure transducer, model XPM60, and a digital pressure calibrator, model PC106, from Beamax, Finland. Pressure calibrations are traceable to National Standards (Center for Metrology and Accreditation Cert. No. M-95P077, 14.11.1995, M-M 730, 16.11.1995, and M-95P078, 16.11.1995): the calibrator uncertainty was 0.0005 MPa; the sensor uncertainty was 0.001 MPa; and the measurement uncertainty was 0.001 MPa. Therefore, the total uncertainty of the pressure measurement is estimated to be within 0.001 MPa.

The vapor and liquid phases in the equilibrium cell were continuously recirculated by a dual-head circulation pump from the Milton Roy Company to reach the equilibrium state rapidly

* Corresponding author: limjs@sogang.ac.kr.

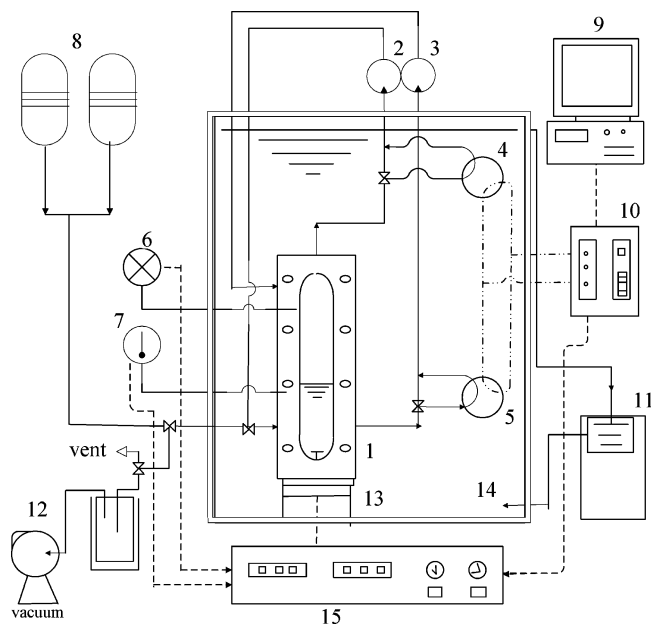


Figure 1. Schematic diagram of the experimental apparatus: (1) equilibrium cell; (2) vapor circulation pump; (3) liquid circulation pump; (4) liquid sample valve; (5) vapor sample valve; (6) temperature indicator; (7) pressure indicator; (8) sample reservoir; (9) computer; (10) gas chromatograph; (11) circulator; (12) vacuum pump; (13) magnetic stirrer; (14) constant temperature water bath; (15) display and controller.

in the cell. The composition of the phases was determined by means of a gas chromatograph of Gow-Mac model 550P connected online to the VLE cell. The response of the thermal conductivity detector (TCD) was carefully calibrated using the mixture prepared gravimetrically and the gas chromatographers (GC) with a Porapak Q column from the Alltech Company. Data derived from gas chromatography were treated with a computer program (Autochro-WIN from Young-Lin Instrument Co., Ltd.)

2.3. Experimental Procedures. Experiments to measure VLE data for the binary system of HFC-134a (1) + *n*-butane (2) at various temperatures were performed by the following procedures. The system was first evacuated to remove all inert gases. A certain amount of *n*-butane was supplied to the cell, and then the temperature of the entire system was held constant by controlling the temperature of the water bath. An open space is required to handle normal butane, and it should be away from any possible ignition because it is flammable. These experiments were conducted within a well-ventilated lab. After the desired temperature was attained, the pressure of the pure component was measured. A proper amount of HFC-134a was introduced into the cell from a sample reservoir. The mixture in the cell was stirred continuously with the magnetic stirrer for 1 h. Both the vapor and liquid phases were recirculated by the dual-head circulation pump until an equilibrium state was established. It is believed that 1 h is sufficient to obtain thermal equilibrium between the cell fluid and the thermostatic bath as well as the vapor and liquid phases. After equilibration, the pressure in the equilibrium cell was measured, and then vapor and liquid samples were withdrawn from the recycling lines by the vapor and liquid sampling valves. The compositions of the samples were measured by immediately injecting them into the GC, which was connected online to the vapor and liquid sampling valves. The GC was calibrated with pure components of known purity and with mixtures of known composition that were prepared gravimetrically. Figure 2 shows the calibration curve.

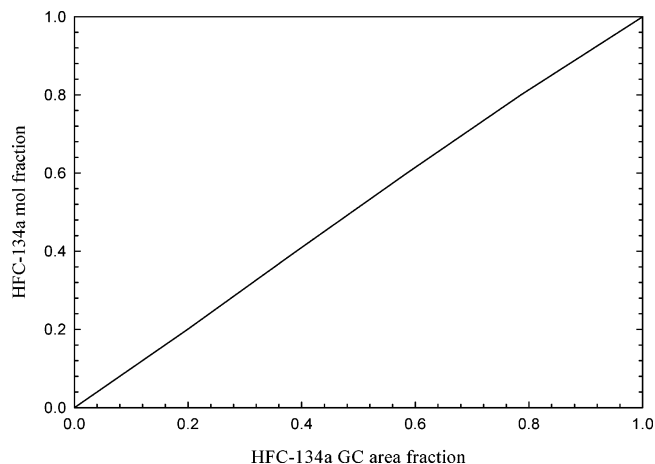


Figure 2. Calibration curve of HFC-134a (1) + *n*-butane (2). The equation of the fitting line for HFC-134a is mole fraction = $-0.0506x(\text{area})^2 + 1.0569(\text{area}) - 0.0034$.

Table 1. Characteristic Properties of the Chemicals (Critical Temperature T_c , Critical Pressure P_c , Acentric Factor ω) from Database REFPROP 6.01¹⁶

component	chemical formula	molecular weight	T_c /K	P_c /MPa	ω
HFC-134a (1)	CF ₃ CH ₂ F	102.03	374.21	4.059	0.3268
<i>n</i> -butane (2)	C ₄ H ₁₀	58.1	425.16	3.796	0.1995

At least five analyses were performed for each phase, and the average values were considered to correspond to the equilibrium values. Considering the margin of error and the reproducibility of the GC, we generally estimated an overall uncertainty in the measurements of the composition of 0.002 mole fractions for both the liquid and the vapor phases.

3. Correlation

The experimental VLE data were correlated with the PR EOS.⁵

$$P = \frac{RT}{v_M - b} - \frac{a(T)}{v_M(v_M + b) + b(v_M - b)} \quad (1)$$

with

$$a(T) = \left(0.457235 \frac{R^2 T_c^2}{P_c}\right) \alpha(T) \quad (2)$$

$$b = 0.077796 \frac{RT_c}{P_c} \quad (3)$$

$$\alpha(T) = [1 + k(1 - \sqrt{T/T_c})]^2 \quad (4)$$

$$k = 0.37464 + 1.54226\omega - 0.26992\omega^2 \quad (5)$$

where the parameter a is a function of temperature; b is constant; k is a constant characteristic of each substance; ω is the acentric factor; P (MPa) is the pressure; P_c (MPa) is the critical pressure; T (K) is the absolute temperature; T_c (K) is the critical temperature; and v_M is the molar volume of the mixture.

The Wong–Sandler (W–S) mixing rules⁶ were used in this work to obtain EOS parameters for a mixture from those of the

Table 2. Pressure of Comparison of the Measured Pure Component Vapor Pressures, P_{exptl} , with Reference Vapor Pressures, P_{REFPROP} , From the Database REFPROP 6.01¹⁶

T K	HFC-134a				n -butane			
	P_{exptl}	P_{REFPROP}	ΔP	$ \Delta P/P $	P_{exptl}	P_{REFPROP}	ΔP	$ \Delta P/P $
	MPa	MPa	MPa		MPa	MPa	MPa	
273.15	0.2928	0.2928	0.0000	0.0000	0.1034	0.1034	0.0000	0.0000
283.15	0.4146	0.4146	0.0000	0.0000	0.1490	0.1487	0.0003	0.0020
293.15	0.5720	0.5717	0.0003	0.0005	0.2083	0.2081	0.0002	0.0010
303.15	0.7702	0.7702	0.0000	0.0000	0.2840	0.2840	0.0000	0.0000
313.15	1.0136	1.0166	-0.0030	0.0030	0.3781	0.3793	-0.0012	0.0032
323.15	1.3128	1.3179	-0.0051	0.0039	0.4931	0.4967	-0.0036	0.0073

Table 3. Vapor–Liquid Equilibrium Measurements for the HFC-134a (1) + n -Butane (2) System at 273.15 to 283.15 K

experimental data			PR EOS (W–S)				experimental data			PR EOS (W–S)			
P_{exptl}			P_{calcd}	ΔP^a		Δy_1^b	P_{exptl}			P_{calcd}	ΔP^a		Δy_1^b
MPa	$x_{1,\text{exptl}}$	$y_{1,\text{exptl}}$	MPa	$y_{1,\text{calcd}}$	MPa		MPa	$x_{1,\text{exptl}}$	$y_{1,\text{exptl}}$	MPa	$y_{1,\text{calcd}}$	MPa	
273.15 K													
0.1034	0.0000	0.0000	0.1035	0.0000	−0.0001	0.0000	0.1490	0.0000	0.0000	0.1486	0.0000	0.0004	0.0000
0.1768	0.0425	0.3113	0.1748	0.4130	0.0020	−0.1017	0.2522	0.0540	0.3164	0.2509	0.4146	0.0013	−0.0983
0.2297	0.1023	0.4747	0.2325	0.5664	−0.0028	−0.0917	0.2752	0.0718	0.3874	0.2752	0.4689	0.0000	−0.0815
0.2750	0.1976	0.5776	0.2759	0.6451	−0.0009	−0.0675	0.3120	0.1066	0.4634	0.3130	0.5382	−0.0010	−0.0748
0.3024	0.3265	0.6456	0.3008	0.6863	0.0016	−0.0407	0.3797	0.2181	0.5824	0.3818	0.6352	−0.0021	−0.0528
0.3137	0.4385	0.6669	0.3128	0.7092	0.0009	−0.0423	0.4180	0.3415	0.6532	0.4161	0.6787	0.0019	−0.0255
0.3239	0.5501	0.7058	0.3214	0.7305	0.0025	−0.0247	0.4358	0.4466	0.7068	0.4329	0.7031	0.0029	0.0037
0.3278	0.6399	0.7342	0.3264	0.7487	0.0015	−0.0145	0.4478	0.5594	0.7241	0.4457	0.7271	0.0021	−0.0030
0.3296	0.7671	0.7781	0.3300	0.7803	−0.0004	−0.0022	0.4513	0.6443	0.7344	0.4527	0.7466	−0.0014	−0.0123
0.3300	0.7999	0.7936	0.3301	0.7909	−0.0001	0.0027	0.4526	0.7454	0.7737	0.4579	0.7749	−0.0053	−0.0013
0.3284	0.8303	0.8034	0.3296	0.8026	−0.0012	0.0008	0.4560	0.7779	0.7874	0.4586	0.7863	−0.0026	0.0011
0.3254	0.8626	0.8261	0.3282	0.8179	−0.0028	0.0082	0.4580	0.8132	0.8030	0.4584	0.8007	−0.0004	0.0023
0.3235	0.8948	0.8500	0.3256	0.8379	−0.0021	0.0121	0.4572	0.8416	0.8203	0.4575	0.8146	−0.0003	0.0057
0.3176	0.9483	0.9061	0.3158	0.8912	0.0018	0.0149	0.4546	0.8864	0.8516	0.4537	0.8426	0.0009	0.0090
0.2928	1.0000	1.0000	0.2921	1.0000	0.0007	0.0000	0.4453	0.9485	0.9139	0.4140	0.9042	0.0052	0.0097
							0.4146	1.0000	1.0000	0.4136	1.0000	0.0010	0.0000

$$^a \Delta P = P_{\text{exptl}} - P_{\text{calcd}}; \quad ^b \Delta y = y_{\text{exptl}} - y_{\text{calcd}}.$$

Table 4. Vapor–Liquid Equilibrium Measurements for the HFC-134a (1) + n -Butane (2) System at 293.15 to 303.15 K

experimental data			PR EOS (W–S)				experimental data			PR EOS (W–S)			
P_{exptl}			P_{calcd}	ΔP^a		Δy_1^b	P_{exptl}			P_{calcd}	ΔP^a		Δy_1^b
MPa	$x_{1,\text{exptl}}$	$y_{1,\text{exptl}}$	MPa	$y_{1,\text{calcd}}$	MPa		MPa	$x_{1,\text{exptl}}$	$y_{1,\text{exptl}}$	MPa	$y_{1,\text{calcd}}$	MPa	
293.15 K													
0.2083	0.0000	0.0000	0.2077	0.0000	0.0007	0.0000	0.2840	0.0000	0.0000	0.2833	0.0000	0.0007	0.0000
0.3211	0.0457	0.2625	0.3189	0.3513	0.0022	−0.0888	0.4153	0.0438	0.2572	0.4122	0.3135	0.0031	−0.0563
0.3764	0.0798	0.3881	0.3778	0.4559	−0.0014	−0.0678	0.5689	0.1326	0.4823	0.5735	0.5157	−0.0046	−0.0334
0.4828	0.1863	0.5369	0.4856	0.5888	−0.0028	−0.0519	0.6686	0.2342	0.5797	0.6697	0.5980	−0.0011	−0.0183
0.5410	0.3010	0.6148	0.5410	0.6445	0.0000	−0.0297	0.7364	0.3589	0.6381	0.7335	0.6495	0.0029	−0.0114
0.5745	0.4032	0.6536	0.5707	0.6761	0.0038	−0.0225	0.7700	0.4577	0.6749	0.7667	0.6799	0.0033	−0.0050
0.5940	0.4977	0.6842	0.5911	0.7017	0.0029	−0.0175	0.7894	0.5359	0.7014	0.7874	0.7031	0.0020	−0.0017
0.6062	0.5847	0.7155	0.6059	0.7257	0.0003	−0.0102	0.8044	0.6203	0.7295	0.8055	0.7297	−0.0011	−0.0002
0.6180	0.6833	0.7495	0.6182	0.7557	−0.0002	−0.0063	0.8164	0.7022	0.7587	0.8186	0.7593	−0.0022	−0.0006
0.6202	0.7719	0.7881	0.6242	0.7884	−0.0040	−0.0003	0.8224	0.7771	0.7939	0.8253	0.7922	−0.0029	0.0017
0.6208	0.8051	0.8050	0.6247	0.8032	−0.0039	0.0018	0.8248	0.8120	0.8126	0.8261	0.8106	−0.0013	0.0020
0.6206	0.8327	0.8207	0.6240	0.8172	−0.0034	0.0035	0.8244	0.8384	0.8305	0.8253	0.8264	−0.0009	0.0041
0.6192	0.8881	0.8588	0.6188	0.8526	0.0004	0.0062	0.8182	0.8990	0.8716	0.8175	0.8712	0.0007	0.0004
0.6110	0.9467	0.9163	0.6032	0.9095	0.0078	0.0068	0.8026	0.9553	0.9311	0.7984	0.9307	0.0042	0.0004
0.5720	1.0000	1.0000	0.5708	1.0000	0.0012	0.0000	0.7702	1.0000	1.0000	0.7698	1.0000	0.0004	0.0000

$$^a \Delta P = P_{\text{exptl}} - P_{\text{calcd}}; \quad ^b \Delta y = y_{\text{exptl}} - y_{\text{calcd}}.$$

pure components. These mixing rules for a cubic equation of state can be written as

$$b_m = \frac{\sum_i \sum_j x_i x_j (b - a/RT)_{ij}}{(1 - A_\infty^E/CRT - \sum_i x_i a_i/RTb_i)} \quad (6)$$

with

$$(b - a/RT)_{ij} = \frac{1}{2}[(b - a/RT)_i + (b - a/RT)_j](1 - k_{ij}) \quad (7)$$

and

$$\frac{a_m}{b_m} = \sum_i x_i \frac{a_i}{b_i} + \frac{A_\infty^E}{C} \quad (8)$$

where C is a numerical constant equal to $\ln(\sqrt{2} - 1)/\sqrt{2}$ for the PR EOS used in this work. The single adjustable parameter

Table 5. Vapor–Liquid Equilibrium Measurements for the HFC-134a (1) + *n*-Butane (2) System at 313.15 to 323.15 K

experimental data			PR EOS (W–S)				experimental data			PR EOS (W–S)			
P_{exptl}			P_{calcd}		ΔP^a		P_{exptl}			P_{calcd}		ΔP^a	
MPa	$x_{1,\text{exptl}}$	$y_{1,\text{exptl}}$	MPa	$y_{1,\text{calcd}}$	MPa	Δy_1^b	MPa	$x_{1,\text{exptl}}$	$y_{1,\text{exptl}}$	MPa	$y_{1,\text{calcd}}$	MPa	Δy_1^b
313.15 K							323.15 K						
0.3781	0.0000	0.0000	0.3784	0.0000	−0.0003	0.0000	0.4931	0.0000	0.0000	0.4958	0.0000	−0.0027	0.0000
0.5260	0.0414	0.2535	0.5202	0.2721	0.0058	−0.0186	0.6428	0.0339	0.2064	0.6344	0.2152	0.0084	−0.0089
0.7012	0.1228	0.4399	0.7083	0.4733	−0.0071	−0.0334	0.8628	0.1149	0.4047	0.8708	0.4339	−0.0080	−0.0292
0.8488	0.2337	0.5657	0.8513	0.5768	−0.0025	−0.0111	1.0554	0.2249	0.5352	1.0594	0.5495	−0.0040	−0.0143
0.9378	0.3481	0.6287	0.9344	0.6314	0.0034	−0.0027	1.1718	0.3349	0.6103	1.1712	0.6100	0.0006	0.0003
0.9946	0.4668	0.6758	0.9911	0.6731	0.0035	0.0026	1.2546	0.4484	0.6604	1.2491	0.6556	0.0055	0.0048
1.0246	0.5522	0.7081	1.0222	0.7018	0.0024	0.0063	1.3056	0.5449	0.6986	1.2995	0.6917	0.0061	0.0069
1.0476	0.6342	0.7389	1.0463	0.7313	0.0013	0.0076	1.3380	0.6313	0.7301	1.3355	0.7260	0.0025	0.0041
1.0650	0.7239	0.7732	1.0655	0.7689	−0.0005	0.0043	1.3646	0.7299	0.7736	1.3653	0.7717	−0.0007	0.0019
1.0716	0.7842	0.8004	1.0728	0.7994	−0.0012	0.0010	1.3704	0.7732	0.7960	1.3736	0.7953	−0.0032	0.0007
1.0734	0.8089	0.8146	1.0741	0.8137	−0.0007	0.0009	1.3762	0.8073	0.8157	1.3774	0.8160	−0.0011	−0.0003
1.0736	0.8309	0.8281	1.0742	0.8275	−0.0005	0.0006	1.3800	0.8352	0.8338	1.3783	0.8347	0.0017	−0.0010
1.0686	0.8912	0.8729	1.0679	0.8726	0.0007	0.0003	1.3670	0.9035	0.8865	1.3702	0.8894	−0.0032	−0.0029
1.0428	0.9502	0.9310	1.0489	0.9315	−0.0060	−0.0005	1.3496	0.9492	0.9308	1.3539	0.9355	−0.0043	−0.0047
1.0136	1.0000	1.0000	1.0177	1.0000	−0.0041	0.0000	1.3128	1.0000	1.0000	1.3216	1.0000	−0.0088	0.0000

$$^a \Delta P = P_{\text{exptl}} - P_{\text{calcd}}. \quad ^b \Delta y = y_{\text{exptl}} - y_{\text{calcd}}.$$

Table 6. Optimal Values of the Binary Parameter, k_{12} , Adjustable Parameters for the NRTL Model, A_{12} and A_{21} , and Absolute Average Deviations of P and y

T K	PR EOS				
	k_{12}	A_{12} kJ·mol ^{−1}	A_{21} kJ·mol ^{−1}	δP^a %	δy^b
273.15	−0.0421	1.9516	2.5510	0.514	0.0283
283.15	0.0276	1.6283	2.1316	0.441	0.0238
293.15	−0.0015	1.6283	2.1485	0.439	0.0209
303.15	0.0796	1.1457	1.6133	0.317	0.0090
313.15	0.1419	1.3212	1.1215	0.324	0.0060
323.15	0.1904	1.2903	0.8789	0.402	0.0053
total average deviation				0.406	0.0156
temperature-dependent parameters				$k_{12} = 0.0046T - 1.3129$	
				$A_{12} = -0.014T + 5.75$	
				$A_{21} = -0.0341T + 11.854$	

$$^a \delta P = 1/N \sum |(P_{\text{exptl}} - P_{\text{calcd}})/P_{\text{exptl}}| \cdot 100. \quad ^b \delta y = 1/N \sum |y_{\text{exptl}} - y_{\text{calcd}}|.$$

(k_{ij}) for each binary pair is referred to as the Wong–Sandler mixing rule parameter. Also, A_{∞}^E is an excess Helmholtz free-energy model at infinite pressure that can be equated to a low-pressure excess Gibbs energy model.¹⁴ In this study, we used the nonrandom two-liquid (NRTL) model¹⁵ given by

$$\frac{A_{\infty}^E}{RT} = \sum_i x_i \frac{\sum_j x_j G_{ji} \tau_{ji}}{\sum_r x_r G_{ri}} \quad (9)$$

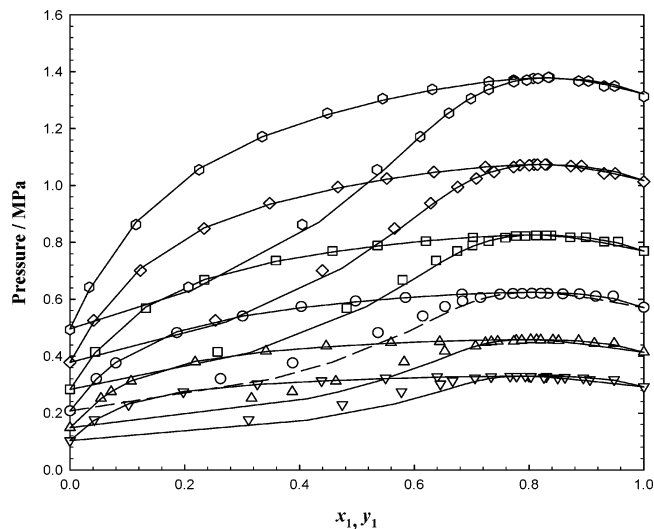
with

$$G_{ji} = \exp(-\alpha_{ji} \tau_{ji}) \text{ and } \tau_{ji} = (g_{ji} - g_{ii})/(RT) \quad (10)$$

where

$$A_{ij} = (g_{ij} - g_{ji}) \quad (11)$$

The critical temperature (T_c), critical pressure (P_c), and acentric factor (ω) for both HFC-134a and *n*-butane that were used to calculate the parameters for the PR EOS are provided in Table 1. We have set the nonrandomness parameter, α_{ij} , equal to a fixed value of 0.3 for all of the binary mixtures studied here. The parameters of the PR EOS were obtained by

**Figure 3.** P – x – y diagram for the HFC-134a (1) + *n*-butane (2) system. Experimental data at: ▽, 273.15; △, 283.15; ○, 293.15; □, 303.15; ◇, 313.15; ○, 323.15 K; —, calculated with the PR EOS using W–S mixing.

minimizing the following objective function.

$$\text{objective function} = \frac{1}{N} \sum_j \left[\left(\frac{P_{j,\text{exptl}} - P_{j,\text{calcd}}}{P_{j,\text{exptl}}} \right) \cdot 100 \right]^2 \quad (12)$$

4. Results and Discussion

Table 2 shows the comparison of measured vapor pressures of pure HFC-134a and *n*-butane with those calculated from the database REFPROP 6.01,¹⁶ which are considered to be reliable for the pure compounds considered and consistent with other literature data. The average deviations ($|\Delta P/P|$ %) between measured and calculated values from REFPROP 6.01 are 0.12 % for HFC-134a and 0.23 % for *n*-butane. The experimental isothermal VLE data for the binary system of HFC-134a + *n*-butane are shown in Tables 3, 4, and 5. These tables list the measured mole fractions of the liquid and vapor phases, pressures, and temperatures in equilibrium and the deviations between measured and calculated pressures (ΔP) and vapor compositions (Δy). The interaction parameters of the binary mixtures for each isotherm, the binary parameters of the NRTL model with the Wong–Sandler mixing rules, and the average

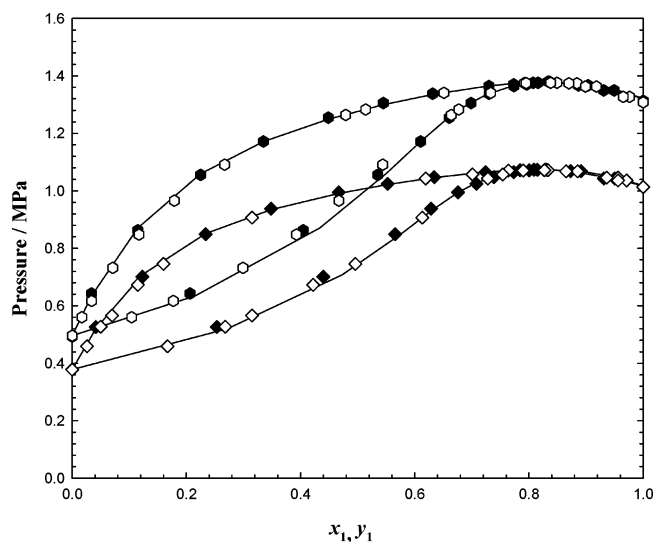


Figure 4. Comparison between the present VLE data (white) with Im et al.'s work (black)⁴ for HFC-134a (1) + *n*-butane (2) at: \diamond , 313.15; \circ , 283.15; \triangle , 293.15; \square , 303.15; \diamond , 313.15; \circ , 323.15 K.

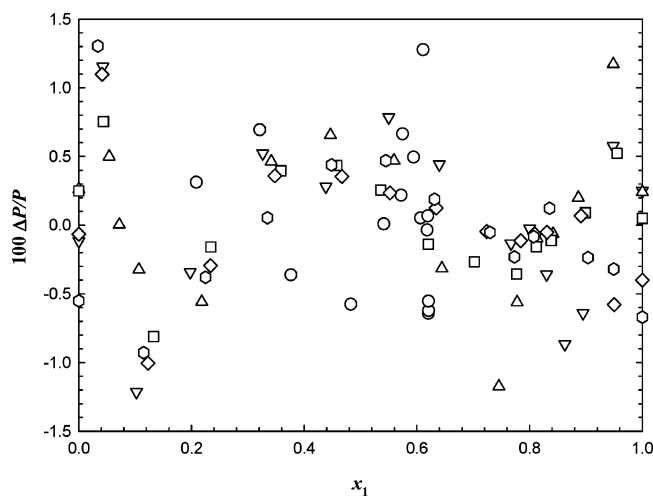


Figure 5. Deviation of pressure for the system HFC-134a (1) + *n*-butane (2) from the PR EOS using the W-S mixing rule at: ∇ , 273.15; \triangle , 283.15; \circ , 293.15; \square , 303.15; \diamond , 313.15; \circ , 323.15 K.

absolute deviations of pressure (δP) and vapor-phase composition (δy) between measured and calculated values are reported in Table 6. These parameters show temperature dependency because they were calculated to reduce AAD P and y . It could be inconvenient to use each parameter depending on each temperature in the industrial level. However, it is difficult to find only one binary interaction parameter for the system because the parameters were temperature dependent. Except two parameters, other parameters showed regular temperature dependency, so they can be fitted with first-order equations for the temperature-dependent binary parameters and adjustable parameters of the NRTL model. The first-order equations are shown at the bottom of Table 6.

Figure 3 shows the comparison of measured and calculated values with the PR EOS for HFC-134a + *n*-butane at 273.15, 283.15, 293.15, 303.15, 313.15, and 323.15 K. The symbols represent the experimental data, and the solid lines and dashed lines show the calculated values of vapor and liquid by the PR EOS, respectively. Both experimental and calculated diagrams clearly indicated that the mixture of HFC-134a and *n*-butane exhibits a positive deviation from Raoult's law as well as

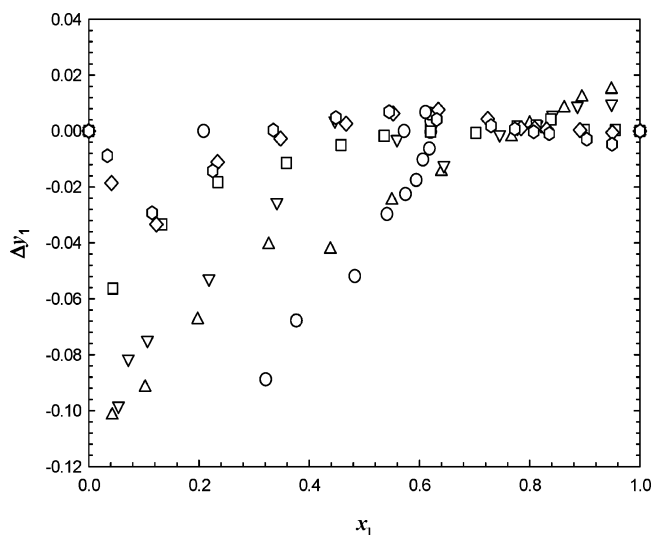


Figure 6. Deviation of vapor composition for the system HFC-134a (1) + *n*-butane (2) from the PR EOS using the W-S mixing rule at: ∇ , 273.15; \triangle , 283.15; \circ , 293.15; \square , 303.15; \diamond , 313.15; \circ , 323.15 K.

Table 7. Azeotropic Data (Azeotropic Pressure, P_{azeo} , Azeotropic Liquid Mole Fraction, x_{azeo}) for the HFC-134a (1) + *n*-Butane (2) System

T/K	$P_{\text{azeo}}/\text{MPa}$	x_{azeo} (HFC-134a mole fraction)
273.15	0.3310	0.7930
283.15	0.4590	0.8000
293.15	0.6209	0.8049
303.15	0.8249	0.8127
313.15	1.0737	0.8180
323.15	1.3810	0.8230

azeotropic behavior. Figure 4 shows the comparison of measured VLE data with literature data reported by Im et al.⁴ for the HFC-134a (1) + *n*-butane (2) system at 313.15 and 323.15 K. The average values of AAD $|\Delta P/P|$ (%) and AAD y were 0.41 % and 0.016 for the PR EOS. The PR EOS-based results are shown in Figures 5 and 6. From these figures and the low average deviations of P and y , we conclude that the calculated values using the PR EOS give good agreement with the experimental data.

This mixture exhibits azeotropes. Azeotropic data for this mixture have been determined at the composition between 0.79 and 0.83 mole fractions and at pressures between 0.331 and 1.38 MPa in the temperature range from 273.15 to 323.15 K.

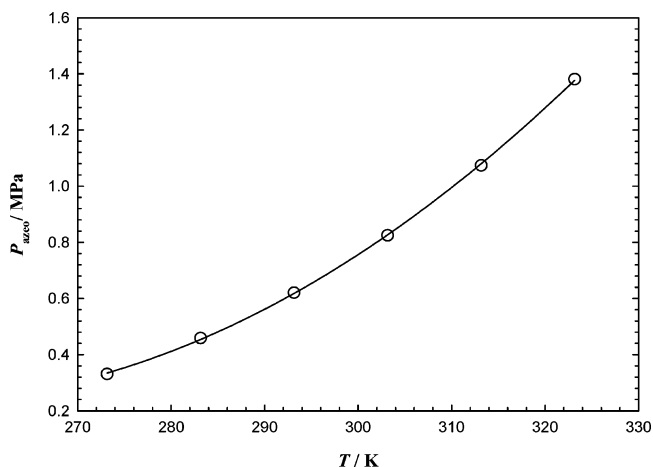


Figure 7. Variation of the azeotropic pressure with temperature for the HFC-134a (1) + *n*-butane (2) system. The equation of the fitting line is $P_{\text{azeo}} = 0.0002T^2 - 0.1117T + 14.261$ ($323.15 \text{ K} \geq T \geq 273.15 \text{ K}$).

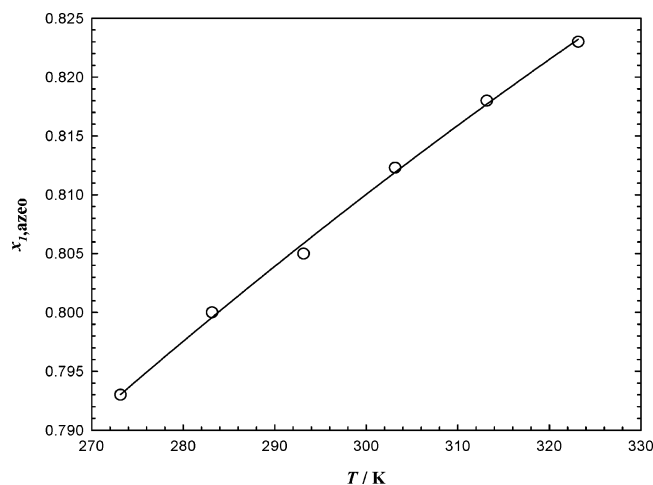


Figure 8. Variation of the azeotropic composition with temperature for the HFC-134a (1) + *n*-butane (2) system. The equation of the fitting line is $x_{1,\text{azeo}} = 0.0006T + 0.6286$ ($323.15 \text{ K} \geq T \geq 273.15 \text{ K}$).

Azeotropic compositions and pressures are shown in Table 7 and Figures 7 and 8. As can be seen in these figures, azeotropic compositions and pressures are dependent on the temperature. In the range of experimental temperatures, azeotropic compositions were correlated by the empirical equation $x_{1,\text{azeo}} = 0.0006T + 0.6286$, and azeotropic pressures were correlated by the empirical equation $P_{\text{azeo}} = 0.0002T^2 - 0.1117T + 14.261$. These equations were fitted within the temperature range $T \geq 273.15 \text{ K}$.

5. Conclusions

VLE data for binary systems of HFC-134a + *n*-butane were measured at six temperatures between 273.15 and 323.15 K using a circulation-type equilibrium apparatus. It is believed that the experimental data are reliable because of good comparison with literature data. The experimental data were correlated with the PR EOS using the Wong–Sandler mixing rules. Calculated results with these equations have given satisfactory results in comparison with the experimental data. This system shows strong positive azeotropes for the full temperature range studied here. These results indicate that the Peng–Robinson equation of state with the Wong–Sandler mixing rules can be used to estimate pressures and compositions for the mixture of HFC-134a + *n*-butane in the range of experimental temperatures and can be applied to other ranges. However, this may need additional experiments to confirm it.

Glossary

$a(T)$	temperature-dependent constant of EOS
A	adjustable parameters
b	molecular volume
g	an energy parameter
k	PR EOS parameter, binary interaction factor
R	gas constant, $8.3144 \text{ (J} \cdot \text{mol}^{-1} \cdot \text{K}^{-1})$
x	liquid mole fraction
y	vapor mole fraction

Greek Letters

α	attraction parameter
Δ	deviation
δ	absolute average deviation
τ	dimensionless form of A/RT

Subscripts

c	critical property
calcd	calculated
exptl	experimental
i, j	i th and j th components of the mixture
azeo	azeotropic point
m	mixtures

Literature Cited

- (1) Poolen, L. J. V.; Holcomb, C. D.; Rainwater, J. C. Isoplethic Method to Estimate Critical Lines for Binary Fluid Mixtures from Subcritical Vapor–Liquid Equilibrium: Application to the Azeotropic Mixtures R32 + C3H8 and R125 + C3H8. *Ind. Eng. Chem. Res.* **2001**, *40*, 4610–4614.
- (2) Kayukawa, Y.; Watanabe, K. $P_p T_x$ Measurements for Gas-Phase Pentafluoroethane + Propane Mixtures by the Burnett Method. *J. Chem. Eng. Data* **2001**, *46* (5), 1025–1030.
- (3) Park, Y. M.; Jung, M. Y. Vapor–Liquid Equilibria for the Pentafluoroethane (HFC-125) + Propane (R-290) System. *J. Chem. Eng. Data* **2002**, *47*, 818–822.
- (4) Im, J. H.; Kim, M.; Lee, B. G.; Kim, H. Vapor–Liquid Equilibria of the Binary *n*-Butane (HC-600) + Difluoromethane (HFC-32), + Pentafluoroethane (HFC-125), + 1,1,1,2-Tetrafluoroethane (HFC-134a) Systems. *J. Chem. Eng. Data* **2005**, *50*, 359–363.
- (5) Peng, D. Y.; Robinson, D. B. A New Two Constant Equation of State. *Ind. Eng. Chem. Fundam.* **1976**, *15*, 59–64.
- (6) Wong, D. S. H.; Sandler, S. I. A Theoretically Correct Mixing Rule for Cubic Equations of State. *AIChE J.* **1992**, *38*, 671–680.
- (7) Lim, J. S.; Park, J. Y.; Lee, B. G.; Lee, Y. W. Phase Equilibria of 1,1,1-Trifluoroethane (HFC-143a) + 1,1,1,2-Tetrafluoroethane (HFC-134a), and + 1,1-Difluoroethane (HFC-152a) at 273.15, 293.15, 303.15, and 313.15 K. *Fluid Phase Equilib.* **2002**, *193*, 29–39.
- (8) Park, J. Y.; Lim, J. S.; Lee, B. G. High-Pressure Vapor–Liquid Equilibria of Binary Mixtures Composed of HFC-32, 125, 134a, 152a, 227ea and R600a (Isobutane). *Fluid Phase Equilib.* **2002**, *194*–197, 981–993.
- (9) Lim, J. S.; Park, J. Y.; Lee, B. G. Phase Equilibria of CFC Alternative Refrigerant Mixtures: 1,1,1,2,3,3,3-Heptafluoropropane (HFC-227ea) + Difluoromethane (HFC-32), 1,1,1,2-Tetrafluoroethane (HFC-134a), and + 1,1-Difluoroethane (HFC-152a). *Int. J. Thermophys.* **2001**, *21*, 1339–1349.
- (10) Lim, J. S.; Park, K. H.; Lee, B. G.; Kim, J. D. Phase Equilibria of CFC Alternative Refrigerant Mixtures. Binary Systems of Trifluoromethane (HFC-23) + 1,1,1,2-Tetrafluoroethane (HFC-134a), and Trifluoromethane (HFC-23) + 1,1,1,2,3,3,3-Heptafluoropropane (HFC-227ea) at 283.15 and 293.15 K. *J. Chem. Eng. Data* **2001**, *46*, 1580–1583.
- (11) Park, J. Y.; Lim, J. S.; Lee, B. G.; Lee, Y. W. Phase Equilibria of CFC Alternative Refrigerant Mixtures: 1,1,1,2,3,3,3-Heptafluoropropane (HFC-227ea) + Difluoromethane (HFC-32), + 1,1,1,2-Tetrafluoroethane (HFC-134a), and + 1,1-Difluoroethane (HFC-152a). *Int. J. Thermophys.* **2001**, *22*, 901–917.
- (12) Lim, J. S.; Park, J. Y.; Lee, B. G. Vapor–Liquid Equilibria of CFC Alternative Refrigerant Mixtures: Trifluoromethane (HFC-23) + Difluoromethane (HFC-32), Trifluoromethane (HFC-23) + Pentafluoroethane (HFC-125), and Pentafluoroethane (HFC-125) + 1,1-Difluoroethane (HFC-152a). *Int. J. Thermophys.* **2000**, *21*, 1339–1349.
- (13) Lim, J. S.; Park, J. Y.; Lee, B. G.; Kim, J. D. Phases Equilibria of CFC Alternative Refrigerant Mixtures. Binary Systems of Trifluoromethane + Isobutane at 283.15 and 293.15 K and 1,1,1-Trifluoroethane + Isobutane at 323.15 and 333.15 K. *J. Chem. Eng. Data* **2000**, *45*, 734–737.
- (14) Wong, D. S. H.; Orbey, H.; Sandler, S. I. Equation of state mixing rule for nonideal mixtures using available activity coefficient model parameters and that allows extrapolation over large ranges of temperature and pressure. *Ind. Eng. Chem. Res.* **1992**, *31*, 2033–2039.
- (15) Renon, H.; Prausnitz, J. M. Local Composition in Thermodynamic Excess Functions for Liquid Mixtures. *AIChE J.* **1968**, *14*, 135–144.
- (16) McLinden, M. O.; Klein, S. A.; Lemmon, E. W.; Peskin, A. P. *Thermodynamic Properties of Refrigerants and Refrigerant Mixtures Database*, REFPROP V.6.01, NIST, 1998.

Received for review January 29, 2007. Accepted March 14, 2007. This research was supported by Sogang University Research Grant in 2007.

JE700041V